Hybrid optomechanical superconducting qubit system

Juuso Manninen [1], Robert H. Blick [2,3] and Francesco Massel [1,*]

[1]*Department of Science and Industry Systems, University of South-Eastern Norway, PO Box 235, Kongsberg, Norway*
[2]*Center for Hybrid Nanostructures (CHyN), Universität Hamburg, Luruper Chaussee 149, 22761 Hamburg, Germany*
[3]*Materials Science and Engineering, University of Wisconsin-Madison, 1509 University Avenue, Wisconsin 53706, USA*

(Received 8 September 2023; accepted 16 February 2024; published 5 April 2024)

We propose an integrated nonlinear superconducting device based on a nanoelectromechanical shuttle. The system can be described as a qubit coupled to a bosonic mode. The topology of the circuit gives rise to an adjustable qubit-mechanical coupling, allowing the experimenter to tune between linear and quadratic coupling in the mechanical degrees of freedom. Owing to its flexibility and potential scalability, the proposed setup represents an important step towards the implementation of bosonic error correction with mechanical elements in large-scale superconducting circuits. We give preliminary evidence of this possibility by discussing a simple state-swapping protocol that uses this device as a quantum memory element.

DOI: 10.1103/PhysRevResearch.6.023029

I. INTRODUCTION

In recent years, optomechanical systems, both in the optical and in the microwave regime, have become one of the most prominent platforms for the investigation of quantum mechanical phenomena. On the one hand, they have allowed scientists to explore foundational aspects of quantum theory [1,2]; on the other, they have provided the test bed for future technological applications of quantum mechanics [3]. Prominent results in the field include sideband [4] and feedback [5] cooling to the ground state, squeezing [6,7], and entanglement [8,9] of mechanical resonators. In the context of coupling between qubits and mechanical resonators, the generation of quantum states of mechanical motion was recently realized in high-overtone bulk acoustic-wave resonators (HBARs) where the generation of Fock [10] and cat [11] states was demonstrated.

In most of the examples mentioned above, the optomechanical system consists of a mechanical resonator (e.g. a nanodrum) whose position is parametrically coupled to a photon cavity. One of the outstanding goals in these systems has been the realization of the so-called single-photon strong-coupling limit. In this regime, the parametric coupling energy between a single photon and the mechanical mode becomes comparable to the bare optical cavity linewidth and can therefore significantly alter the dynamics of the system [12–20]. In microwave setups, several proposals suggest that the addition of nonlinear elements, in the form of Josephson junctions, can provide the resource needed to reach the strong-coupling regime; realizations along these lines include charge [12,21] and flux-mediated optomechanical circuits [22].

Another intriguing aspect of these systems is the possibility of realizing a quadratic coupling between the mechanical motion and the optical field. Arguably, its most prominent application is the detection of phonon Fock states [23–27], even though two-photon cooling and squeezing both of the mechanical and the electromagnetic degrees of freedom have been predicted [27] as well. In the optical frequencies range, the quadratic coupling of an optical cavity with a mechanical mode has been realized, e.g., in membrane-in-the-middle [23] and ultracold gases setups [28]. In the microwave regime, quadratic parametric coupling of a qubit to mechanical motion was recently realized with drumhead mechanical resonators coupled to superconducting circuits, exploiting the large mismatch of mechanical and qubit resonant frequency [29,30], where the generation of (non-Gaussian) number-squeezed states was demonstrated.

In this work, we extend the nonlinear circuit approaches mentioned above, integrating a mechanical shuttling element into the design of the superconducting circuit of Fig. 1. The shuttling element consists here of a portion of superconducting material that is free to perform mechanical oscillations between two (superconducting) electrodes. Analogous shuttling devices were realized experimentally in normal (i.e., nonsuperconducting) circuits [31–33], demonstrating the ability of such devices to "shuttle" electrons along with the oscillatory mechanical motion. In addition, an analogous shuttling mechanism for Cooper pairs was theoretically investigated for superconducting circuits [34]. In our work, we explore how the dynamical properties of a superconducting shuttling element can be recast in terms of a (nonlinear) optomechanical coupling between a superconducting circuit and a mechanical mode, for which we believe this particular charge shuttling mechanism certainly offers a new degree of freedom [35].

*francesco.massel@usn.no

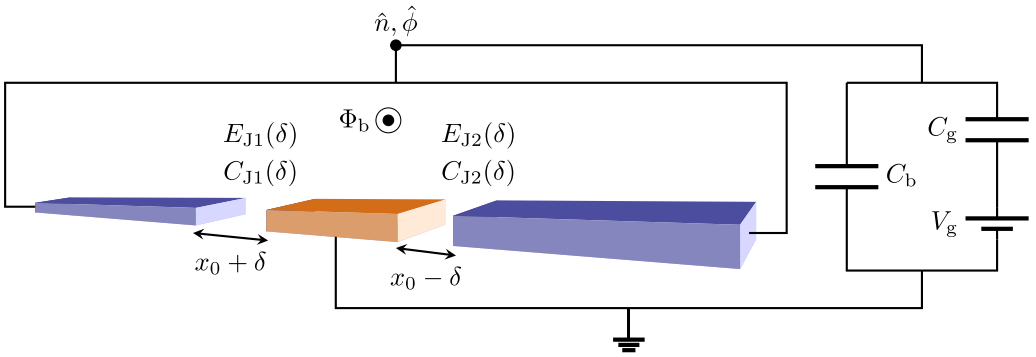

FIG. 1. Cartoon picture of a (grounded) X2MON shuttle and a lumped-element description of a transmon-like setup, including the X2MON. Contacts between the shuttle (orange) and its terminals (blue) can be described by position-dependent Josephson junctions.

More specifically, we show how, in a lumped-element description, we are able to define a system constituted by a superconducting qubit exhibiting an intrinsic quadratic coupling to the mechanical motion, in addition to a tunable linear one. The latter can be externally suppressed, leading to a dominant coupling that is quadratic in the mechanical degrees of freedom. At the same time, we will show that the tunability of the linear coupling term allows for a coherent state exchange between the qubit and the mechanical resonator.

II. THE DEVICE

Our device is constituted by a superconducting shuttle, which is free to oscillate between two terminals, as shown in Fig. 1. The terminals are gated to a voltage source V_g through a gating capacitance C_g. The addition of a shunting capacitance C_b, meant to ensure protection from charge fluctuations, defines a transmon qubit-like device [36] (the X2MON) exhibiting nontrivial properties as a function of the mechanical shuttle dynamics. The displacement of the grounded island induces a shift in the Josephson and charging energies of the two Josephson junctions (JJs), which translates into a coupling between the superconducting circuit and the mechanical motion. As anticipated, in our device, the coupling between the mechanical degrees of freedom and a superconducting qubit can be externally tuned between a *linear* and a *quadratic* coupling, depending on the external magnetic flux through the loop defined by the two JJs. The setup we propose here differs from the design of Refs. [29,30] inasmuch our realization, for suitable values of the control parameter, is *intrinsically* quadratic in the mechanical displacement—i.e., not relying on the relative value of the mechanical and qubit frequencies—owing to the symmetry of the design.

From a quantum-computational perspective, the coupling between a qubit and a bosonic mode—represented here, as we will show, by a shuttling mechanical element—is an extremely promising candidate for quantum error correction [37,38]. Most importantly, the tunability of the qubit-mechanical coupling of our setup allows for a great flexibility in the choice of different protocols for state preparation and statetransfer between qubit and mechanics. Further advantages offered by mechanical resonators compared to microwave cavities as the bosonic mode are represented by their larger coherence times (mechanical linewidths $\sim$1 kHz [32] vs cavity linewidths $\sim$100 kHz), the lack of "crosstalk" between the bosonic (mechanical) modes and, with specific reference to shuttling mechanical elements, the scalability of such platforms.

A. Lumped-element model

Following Koch *et al.* [36], we describe the Josephson junction energy as the sum of a capacitive contribution E_C and the Josephson energy E_J. In our device, the lower portion of the circuit—the orange element in Fig. 1—corresponds to the actual island. As a consequence, the charging and Josephson energies become dependent on the shuttle dynamics $E_{C\,1,2} = E_{C\,1,2}(x_0 \pm \delta)$, $E_{J\,1,2} = E_{J\,1,2}(x_0 \pm \delta)$. Owing to the symmetry of the device, the upper (lower) sign corresponds to junction 1 (junction 2).

The total charging energy for the circuit can be written as

$$E_C = \frac{e^2}{2C_\Sigma} \tag{1}$$

with $C_\Sigma = C_{J1} + C_{J2} + C_b + C_g$, where C_{J1} and C_{J2} are the capacitances of the two Josephson junctions, C_g the gate capacitance, and C_b the shunting capacitance aimed at reducing the effects of charge noise, as in a conventional transmon setup.

In the following, we will assume that the geometric capacitances associated with the Josephson junctions C_{J1} and C_{J2} can be modeled by two (equal, parallel plate) capacitors $C_{J\,1,2} \doteq C_J/(1 \pm \delta/x_0)$. Furthermore, we assume an exponential dependence of E_J on the electrodes' separation. This assumption can be justified through the standard Ambegaokar-Baratoff formula [39,40] arguing that the normal-state resistance is given by $R_N = R_{N0}\exp[x/\xi]$ (x being the thickness of the JJ), as a consequence of the exponential suppression of the tunneling probability through a potential barrier, combined with the Landauer formula [41], leading to

$$E_{J\,1,2} = E_J \exp\left[\mp\frac{\delta}{\xi}\right] \tag{2}$$

with $\xi = x_0/\ln[\frac{\Delta R_K}{8E_J R_{N0}}]$ and $E_J = E_{J1}(0) = E_{J2}(0)$ for symmetrical JJs. Here Δ is the superconducting gap and $R_K = 2\pi\hbar/e^2$ the resistance quantum. For a typical NbN junction, we can assume $\Delta = 4500$ GHz, $E_J = 20$ GHz, $R_{N0} = 50\ \Omega$, and $x_0 = 1$ nm, allowing us to estimate $\xi \simeq 0.1$ nm ($\hbar = 1$

throughout the paper). Following Ref. [36], we can write the system's Hamiltonian as

$$H = 4E_{\rm C}(\delta)(n-n_{\rm g})^2 - E_\Sigma(\delta)\cos\left(\frac{\phi_{\rm b}}{2}\right)\cos(\phi) - E_\Delta(\delta)\sin\left(\frac{\phi_{\rm b}}{2}\right)\sin(\phi) + E(x_{\rm m}, p_{\rm m}), \tag{3}$$

where n and ϕ are the excess number of charge carriers and phase on the island, respectively, and $E_\Sigma(\delta) = E_{\rm J1}(\delta) + E_{\rm J2}(\delta)$, $E_\Delta(\delta) = E_{\rm J1}(\delta) - E_{\rm J2}(\delta)$. For a symmetric setup, we have

$$E_\Sigma(\delta) = 2E_{\rm J}\cosh\left(\frac{\delta}{\xi}\right), \tag{4a}$$

$$E_\Delta(\delta) = 2E_{\rm J}\sinh\left(\frac{\delta}{\xi}\right), \tag{4b}$$

where $E_{\rm J}$ is the Josephson energy associated with either junction. Furthermore, $n_{\rm g}$ is related to the external bias voltage by $n_{\rm g} = -C_{\rm g}V_{\rm g}/2e$ and the phase $\phi_{\rm b}$ is determined by the external flux bias $\Phi_{\rm b} = \Phi_0/2\pi\,\phi_{\rm b}$ through the loop defined by the two JJs ($\Phi_0 = h/2e$). Here, the JJs are assumed to be symmetrical, but the full calculation with general junctions is presented in the Supplemental Material [42]. Finally, the term $E(x_{\rm m}, p_{\rm m})$ in the energy associated with the dynamics of the center of mass of the shuttle, which, in our analysis, we model as a simple harmonic oscillator.

Expanding the Hamiltonian given in Eq. (3) in powers of $\hat{\phi}$ up to the fourth order and in powers of the mechanical displacement up to the second order, and focusing on the two lowest-charge states, we have (see, e.g., [43])

$$H = \frac{\omega_{\rm q}}{2}\sigma_{\rm z} + \omega_{\rm m}b^\dagger b + g_1(b^\dagger + b)\sigma_{\rm x} + g_2(b^\dagger + b)^2\sigma_{\rm z}, \tag{5}$$

where $\sigma_{\rm z} = 2a^\dagger a - 1$, $\sigma_{\rm x} = a^\dagger + a$. The operators a ($a^\dagger$), b ($b^\dagger$) are the lowering (raising) operators associated with the electrical and mechanical degrees of freedom, respectively. All coefficients in Eq. (5) ($\omega_{\rm q}$, $\omega_{\rm m}$, g_1, g_2) depend on the external flux bias. The explicit dependence on $\Phi_{\rm b}$ is given in the Supplemental Material [42]. As shown in Fig. 2, g_2 is the dominating interaction when the bias flux through the JJ loop is set to zero, since g_1 vanishes in this case. However, g_1 becomes the dominating term even for small deviations from the $\Phi_{\rm b} = 0$ condition. As we will show below, this ability to control the type of interaction between the qubit and the mechanics makes this system very flexible in terms of possible applications, such as preparing the mechanical oscillator into a specific quantum state. For $m \simeq 5\times10^{-19}$ kg, $\omega_{\rm m} = 1$ GHz, and $\omega_{\rm q} \simeq 17$ GHz (all other parameters defined above), we have that $x_{\rm ZPF}/\xi \simeq 3\times10^{-3}$, $g_2 \simeq 40$ kHz. Also, note that the Hamiltonian given in Eq. (5) is valid in the case of equal JJs. If the JJs exhibit some degree of asymmetry, a linear coupling to σ_z and a quadratic coupling to $\sigma_{\rm x}$ appear, in addition to a small qubit rotation (zeroth-order term in σ_x). While the quadratic coupling to $\sigma_{\rm x}$ is negligible for all parameters, the linear coupling between the displacement and σ_z becomes comparable to the quadratic one when the asymmetry of the Josephson energies is $\sim\frac{x_{\rm ZPF}}{2\xi}$, which, for the parameters chosen here, corresponds to $\Delta E_{\rm J} = |E_{\rm J1} - E_{\rm J2}| \simeq 30$ MHz. Furthermore, the zeroth-order term in σ_x is negligible whenever the asymmetry $d_0 = |E_{\rm J1} - E_{\rm J2}|/|E_{\rm J1} + E_{\rm J2}|$ is (much) less than unity. A discussion of the general case of different JJs is presented in the Supplemental Material [42].

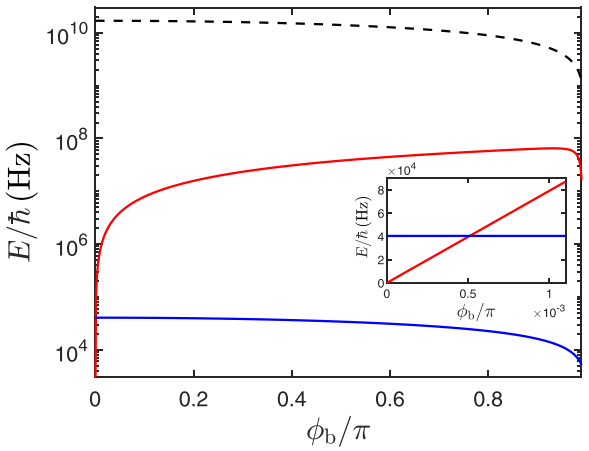

FIG. 2. The strengths of g_1 (red) and g_2 (blue) couplings and the qubit frequency $\omega_{\rm q}$ (dashed black) as a function of the external flux $\phi_{\rm b}$. The inset shows the crossover point near zero flux bias where g_1 becomes larger than g_2. Parameters: $E_{\rm J} = 20$ GHz, $E_{\rm C} = 1$ GHz, $x_{\rm ZPF}/\xi = 3\times10^{-3}$.

III. STATE SWAPPING PROTOCOL

A promising application for the setup proposed here is bosonic error correction. On general grounds, bosonic error correction provides key advantages over quantum error correction schemes utilizing multiple physical qubits, inasmuch it eliminates the overheads and the potential issues arising from crosstalk of multiple physical qubits. More specifically, our mechanical implementation has further advantages over a microwave cavity: mechanical resonators offer better ringdown times than microwave cavities, shuttling resonators offer a more compact design and relatively straightforward scalability, and the qubit-mechanics (linear) coupling can be externally tuned.

As a first step in this direction, we consider a state-swap protocol that demonstrates the ability of this device to coherently transfer a qubit state to a quantum state of the mechanical resonator. Given the relatively large frequency mismatch between the qubit and the mechanics ($\omega_{\rm q}/\omega_{\rm m} \simeq 20$), direct transitions between mechanics and qubit are highly nonresonant. To induce such sideband transitions, we therefore modulate the flux through the JJs loop at a frequency $\bar{\omega}$, corresponding to a phase modulation given by $\phi_{\rm b}(t) = \phi_{\rm b,0}\cos(\bar{\omega}t)$ (flux-driven sideband transitions). This technique is analogous to the one employed in Ref. [44] for the case of a transmon qubit coupled to a microwave cavity. In the context of optomechanical systems, a similar approach was also considered in [30], where the gate charge modulation was used to induce single-phonon transitions in a mechanical resonator coupled to a qubit. In general, these techniques go under the name of ac-dither techniques [45].

As a consequence of the phase modulation, the coefficients appearing in the definition of the Hamiltonian H in Eq. (5)

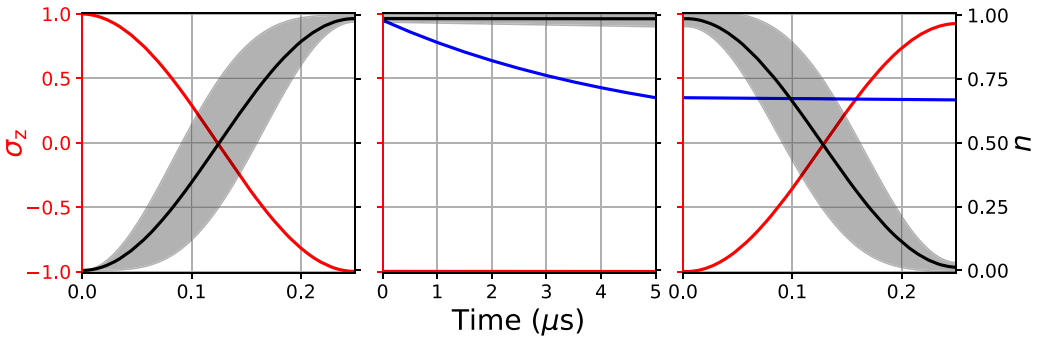

FIG. 3. Demonstration of the state swapping protocol. Left panel: the qubit state $|\sigma_z = 1\rangle$ (red line) is transferred to the mechanical oscillator Fock state $|n = 1\rangle$ (black line/black shade). Central panel: the linear coupling g_1 is suppressed. The free evolution of the state $|n = 1\rangle$ is subject to the (small) intrinsic dissipation of the mechanical resonator. Right panel: the state $|n = 1\rangle$ is transferred back to the qubit. The fidelity of the swapping to the mechanical resonator and back, is compared with the free evolution of the $|\sigma_z = 1\rangle$ state under subject to pure qubit decoherence (blue line). Parameters: $E_C = 1$ GHz, $E_J = 20$ GHz, $x_{ZPF}/\xi = 3 \times 10^{-3}$, $\phi_{b,0} = 0.5$, mechanical angular frequency $\omega_m = 1$ GHz, and damping rate $\gamma = 1$ kHz, qubit damping rate $\gamma_\sigma = 100$ kHz. In the simulations, we have assumed a finite temperature of 10 mK, both for the qubit and for the mechanical bath, corresponding to populations of $n_{\sigma,th} \simeq 2 \times 10^{-7}$ and $n_{m,th} \simeq 0.87$, respectively. The time axis is reset to zero for each step in the protocol to better illustrate the different timescales.

become time dependent:

$$H = \frac{\omega_q(t)}{2}\sigma_z + \omega_m(t)b^\dagger b + g_1(t)(b^\dagger + b)\sigma_x + g_2(t)(b^\dagger + b)^2\sigma_z. \quad (6)$$

It is possible to show that, in a nonuniformly rotating frame for the qubit and the mechanics, if the driving frequency is chosen in such a way that $\bar{\omega} = \bar{\omega}_q - \omega_m$, with $\bar{\omega}_q = \omega_q|_{\phi_b=0} - \delta_q$, $\delta_q = \phi_{b,0}^2\omega_{p0}/16$, and $\omega_{p0} = \sqrt{16E_C E_J \cos(\phi_b/2)}$ for symmetrical JJs, the transformed Hamiltonian corresponds to a state-swapping Hamiltonian

$$H' = g_{sw}(b^\dagger\sigma_- + b\sigma_+), \quad (7)$$

where $g_{sw} = \bar{g}_1 J_0(\delta_q/2\bar{\omega})$ with $J_0(x)$ being the zeroth-order Bessel function and $\bar{g}_1$ the linear approximation of $g_1(t)$ with respect to $\phi_{b,0}$.

Given that $\phi_{b,0}$ is externally tunable, after the state-swapping transition described above, it is possible to externally suppress the linear coupling between the qubit and the mechanical resonator. Having this in mind, one can consider using the mechanical mode as a low-decoherence memory element, owing to the combined effect of the on-demand suppression of lowest-order coupling between the qubit and the mechanical resonator, and the intrinsically long decoherence times of the mechanical element.

In Fig. 3, we depict a simple instance of the state-swap protocol. Starting from the state $|\sigma_z = 1, n_m = 0\rangle$, we first perform a state swap between the qubit state and the mechanics (left), followed by the "free" evolution in the absence of qubit-mechanics coupling, $\phi_b = 0$, implying $g_1 = 0$ (center), transferring then the excitation back to the qubit (right). We have compared this state-swapping protocol with the free evolution of the $|\sigma_z = 1\rangle$ state in the presence of the same environment (qubit decay rate $\gamma_\sigma = 100$ kHz) as for the state-swap protocol. The $|\sigma_z = 1, n_m = 0\rangle$ initial state can be prepared resorting to a preliminary cooling step of the mechanical mode. We would like to point out that, while the parameters chosen here push the boundaries of what is experimentally realizable, with values of the fQ product of the order of 10^{14}, record values of $fQ = O(10^{18})$ have been reported for bulk acoustic wave resonators [46,47].

IV. EXPERIMENTAL OUTLOOK AND PERFORMANCE

From an experimental point of view, the realization of a shuttling island (orange box in Fig. 1) can be performed with some additional processing steps. However, fabrication of a superconducting island has turned out to be a challenge so far, since standard superconducting materials, such as Al, tend to oxidize through for small 50^3 nm^3 islands. Our latest work on that end shows that we can realize superconducting NbN strips [48] with a $T_c = 9$ K, which avoids the aforementioned issue and is fully compatible with our processing techniques. Hence, the fabrication of superconducting islands in varying circuit combinations is possible now. One of the circuits to be implemented is shown in Fig. 1.

Additionally, the ability to perform precise ac-dither protocols with the magnetic flux is required to successfully operate the device as a platform for useful quantum operations. These techniques are, in principle, possible with tuning either the gate charge or the magnetic flux [45], and different kinds of modulation schemes have been experimentally demonstrated to be feasible, e.g., Ref. [30] for charge-based and Refs. [44,49] for flux-based procedures.

Note that, in this work, we do not focus on parameter optimization for our device, for example to maximize the couplings or to minimize the noise in the circuit, but instead we use fairly typical values for superconducting circuits. As an example, one could introduce a larger shunting capacitance to avoid charge noise effects thanks to the reduced charging energy, placing the device firmly in the $E_J \gg E_C$ transmon regime.

Even though we are not aiming to optimize the performance of our device here, the accessible coupling strengths between the qubit and the mechanics are promising when considering the proposed device as a candidate for practical quantum computation protocols. We obtain a quadratic

coupling g_2 that is about an order of magnitude larger than presently achievable linewidths for shuttling mechanical resonators using the parameters in Fig. 2 for a wide range of flux biasing, and $g_2/\omega_m \approx 4 \times 10^{-5}$, which is comparable to different state-of-the-art implementations of bosonic error correction schemes. For example, in a recent demonstration of quantum error correction beyond the break-even point using a bosonic (photonic) GKP code [38], the corresponding ratio was $\sim 1 \times 10^{-5}$ with a superconducting cavity as the bosonic system. However, we do not predict reaching the ultrastrong coupling limit as in Ref. [30], but in terms of the linear coupling g_1 we still can attain significantly larger values than the resonator linewidth with $g_1/\omega_m > 0.01$ already starting from a small flux bias.

We want to emphasize that the state swapping protocol explored in this work is not meant to be a comprehensive procedure for bosonic error correction, but instead a proof of concept that our device could be useful in such applications. Indeed, it is possible to create arbitrary phonon number states with detailed control of the state swapping Hamiltonian [50] and, additionally, other interesting and useful operations can be realized with this interaction alone, such as the preparation of mechanical cat states [11]. On top of this linear interaction between the qubit and the mechanics, we also have access to another resource, namely the quadratic coupling, that is largely unexplored in this work.

V. CONCLUSIONS

In our work, we introduce a device (the X2MON) which consists of a transmon coupled to a mechanical shuttle operating in the quantum regime. We discuss the nature of the coupling between the two. Furthermore, we demonstrate a state-swap protocol, which, owing to the properties of the shuttle, can be directly employed as a quantum memory. Our work paves the way for bosonic error correction with mechanical modes.

ACKNOWLEDGMENTS

The numerical simulations were performed using the `QuantumOptics.jl` numerical framework [51]. F.M. and J.M. acknowledge financial support from the Research Council of Norway (Grant No. 333937) through participation in the QuantERA ERA-NET Cofund in Quantum Technologies. R.H.B. acknowledges collaboration with Nexperia GmbH, Germany.

[1] W. Marshall, C. Simon, R. Penrose, and D. Bouwmeester, Towards quantum superpositions of a mirror, Phys. Rev. Lett. **91**, 130401 (2003).

[2] M. Aspelmeyer, T. J. Kippenberg, and F. Marquardt, Cavity optomechanics, Rev. Mod. Phys. **86**, 1391 (2014).

[3] S. Barzanjeh, A. Xuereb, S. Gröblacher, M. Paternostro, C. A. Regal, and E. M. Weig, Optomechanics for quantum technologies, Nat. Phys. **18**, 15 (2022).

[4] J. D. Teufel, T. Donner, D. Li, J. W. Harlow, M. S. Allman, K. Cicak, A. J. Sirois, J. D. Whittaker, K. W. Lehnert, and R. W. Simmonds, Sideband cooling of micromechanical motion to the quantum ground state, Nature (London) **475**, 359 (2011).

[5] M. Rossi, D. Mason, J. Chen, Y. Tsaturyan, and A. Schliesser, Measurement-based quantum control of mechanical motion, Nature (London) **563**, 53 (2018).

[6] E. E. Wollman, C. U. Lei, A. J. Weinstein, J. Suh, A. Kronwald, F. Marquardt, A. A. Clerk, and K. C. Schwab, Quantum squeezing of motion in a mechanical resonator, Science **349**, 952 (2015).

[7] J.-M. Pirkkalainen, E. Damskägg, M. Brandt, F. Massel, and M. A. Sillanpää, Squeezing of quantum noise of motion in a micromechanical resonator, Phys. Rev. Lett. **115**, 243601 (2015).

[8] R. Riedinger, A. Wallucks, I. Marinković, C. Löschnauer, M. Aspelmeyer, S. Hong, and S. Gröblacher, Remote quantum entanglement between two micromechanical oscillators, Nature (London) **556**, 473 (2018).

[9] C. F. Ockeloen-Korppi, E. Damskägg, J.-M. Pirkkalainen, M. Asjad, A. A. Clerk, F. Massel, M. J. Woolley, and M. A. Sillanpää, Stabilized entanglement of massive mechanical oscillators, Nature (London) **556**, 478 (2018).

[10] Y. Chu, P. Kharel, T. Yoon, L. Frunzio, P. T. Rakich, and R. J. Schoelkopf, Creation and control of multi-phonon Fock states in a bulk acoustic-wave resonator, Nature (London) **563**, 666 (2018).

[11] M. Bild, M. Fadel, Y. Yang, U. v. Lüpke, P. Martin, A. Bruno, and Y. Chu, Schrödinger cat states of a 16-microgram mechanical oscillator, Science **380**, 274 (2023).

[12] T. T. Heikkilä, F. Massel, J. Tuorila, R. Khan, and M. A. Sillanpää, Enhancing optomechanical coupling via the Josephson effect, Phys. Rev. Lett. **112**, 203603 (2014).

[13] P. D. Nation, J. Suh, and M. P. Blencowe, Ultrastrong optomechanics incorporating the dynamical Casimir effect, Phys. Rev. A **93**, 022510 (2016).

[14] E. Romero-Sánchez, W. P. Bowen, M. R. Vanner, K. Xia, and J. Twamley, Quantum magnetomechanics: Towards the ultrastrong coupling regime, Phys. Rev. B **97**, 024109 (2018).

[15] L. Neumeier, T. E. Northup, and D. E. Chang, Reaching the optomechanical strong-coupling regime with a single atom in a cavity, Phys. Rev. A **97**, 063857 (2018).

[16] L. Neumeier and D. E. Chang, Exploring unresolved sideband, optomechanical strong coupling using a single atom coupled to a cavity, New J. Phys. **20**, 083004 (2018).

[17] A. Settineri, V. Macrí, A. Ridolfo, O. D. Stefano, A. F. Kockum, F. Nori, and S. Savasta, Dissipation and thermal noise in hybrid quantum systems in the ultrastrong-coupling regime, Phys. Rev. A **98**, 053834 (2018).

[18] M. Kounalakis, Y. M. Blanter, and G. A. Steele, Flux-mediated optomechanics with a transmon qubit in the single-photon ultrastrong-coupling regime, Phys. Rev. Res. **2**, 023335 (2020).

[19] J.-Q. Liao, J.-F. Huang, L. Tian, L.-M. Kuang, and C.-P. Sun, Generalized ultrastrong optomechanical-like coupling, Phys. Rev. A **101**, 063802 (2020).

[20] J. Manninen, M. T. Haque, D. Vitali, and P. Hakonen, Enhancement of the optomechanical coupling and Kerr nonlinearity

using the Josephson capacitance of a Cooper-pair box, Phys. Rev. B **105**, 144508 (2022).
[21] J. M. Pirkkalainen, S. U. Cho, F. Massel, J. Tuorila, T. T. Heikkilä, P. J. Hakonen, and M. A. Sillanpää, Cavity optomechanics mediated by a quantum two-level system, Nat. Commun. **6**, 6981 (2015).
[22] T. Bera, S. Majumder, S. K. Sahu, and V. Singh, Large flux-mediated coupling in hybrid electromechanical system with a transmon qubit, Commun. Phys. **4**, 12 (2021).
[23] J. D. Thompson, B. M. Zwickl, A. M. Jayich, F. Marquardt, S. M. Girvin, and J. G. E. Harris, Strong dispersive coupling of a high-finesse cavity to a micromechanical membrane, Nature (London) **452**, 72 (2008).
[24] A. M. Jayich, J. C. Sankey, B. M. Zwickl, C. Yang, J. D. Thompson, S. M. Girvin, A. A. Clerk, F. Marquardt, and J. G. E. Harris, Dispersive optomechanics: a membrane inside a cavity, New J. Phys. **10**, 095008 (2008).
[25] F. Helmer, M. Mariantoni, E. Solano, and F. Marquardt, Quantum nondemolition photon detection in circuit QED and the quantum Zeno effect, Phys. Rev. A **79**, 052115 (2009).
[26] H. Miao, S. Danilishin, T. Corbitt, and Y. Chen, Standard quantum limit for probing mechanical energy quantization, Phys. Rev. Lett. **103**, 100402 (2009).
[27] A. Nunnenkamp, K. Børkje, J. G. E. Harris, and S. M. Girvin, Cooling and squeezing via quadratic optomechanical coupling, Phys. Rev. A **82**, 021806(R) (2010).
[28] T. P. Purdy, D. W. C. Brooks, T. Botter, N. Brahms, Z.-Y. Ma, and D. M. Stamper-Kurn, Tunable cavity optomechanics with ultracold atoms, Phys. Rev. Lett. **105**, 133602 (2010).
[29] J. J. Viennot, X. Ma, and K. W. Lehnert, Phonon-number-sensitive electromechanics, Phys. Rev. Lett. **121**, 183601 (2018).
[30] X. Ma, J. J. Viennot, S. Kotler, J. D. Teufel, and K. W. Lehnert, Non-classical energy squeezing of a macroscopic mechanical oscillator, Nat. Phys. **17**, 322 (2021).
[31] D. V. Scheible and R. H. Blick, Silicon nanopillars for mechanical single-electron transport, Appl. Phys. Lett. **84**, 4632 (2004).
[32] D. R. Koenig, E. M. Weig, and J. P. Kotthaus, Ultrasonically driven nanomechanical single-electron shuttle, Nat. Nanotechnol. **3**, 482 (2008).
[33] C. Kim, M. Prada, and R. H. Blick, Coulomb blockade in a coupled nanomechanical electron shuttle, ACS Nano **6**, 651 (2012).
[34] L. Y. Gorelik, A. Isacsson, Y. M. Galperin, R. I. Shekhter, and M. Jonson, Coherent transfer of Cooper pairs by a movable grain, Nature (London) **411**, 454 (2001).
[35] C. Kim, R. Marsland, and R. H. Blick, The nanomechanical bit, Small **16**, 2001580 (2020).
[36] J. Koch, T. M. Yu, J. Gambetta, A. A. Houck, D. I. Schuster, J. Majer, A. Blais, M. H. Devoret, S. M. Girvin, and R. J. Schoelkopf, Charge-insensitive qubit design derived from the Cooper pair box, Phys. Rev. A **76**, 042319 (2007).
[37] M. H. Michael, M. Silveri, R. T. Brierley, V. V. Albert, J. Salmilehto, L. Jiang, and S. M. Girvin, New class of quantum error-correcting codes for a bosonic mode, Phys. Rev. X **6**, 031006 (2016).
[38] V. V. Sivak, A. Eickbusch, B. Royer, S. Singh, I. Tsioutsios, S. Ganjam, A. Miano, B. L. Brock, A. Z. Ding, L. Frunzio, S. M. Girvin, R. J. Schoelkopf, and M. H. Devoret, Real-time quantum error correction beyond break-even, Nature (London) **616**, 50 (2023).
[39] V. Ambegaokar and A. Baratoff, Tunneling between superconductors, Phys. Rev. Lett. **10**, 486 (1963).
[40] J. M. Martinis, Course 13: Superconducting qubits and the physics of Josephson junctions, Les Houches **79**, 487 (2004).
[41] R. Landauer, Spatial variation of currents and fields due to localized scatterers in metallic conduction, IBM J. Res. Dev. **1**, 223 (1957).
[42] See Supplemental Material at http://link.aps.org/supplemental/10.1103/PhysRevResearch.6.023029 for detailed derivations of the X2MON Hamiltonian and the state-swap protocol.
[43] S. M. Girvin, Superconducting qubits and circuits: Artificial atoms coupled to microwave photons, in *Quantum Machines: Measurement and Control of Engineered Quantum Systems - Lecture Notes of the Les Houches Summer School*, Vol. 96 (Oxford University Press, Oxford, 2014).
[44] J. D. Strand, M. Ware, F. Beaudoin, T. A. Ohki, B. R. Johnson, A. Blais, and B. L. T. Plourde, First-order sideband transitions with flux-driven asymmetric transmon qubits, Phys. Rev. B **87**, 220505(R) (2013).
[45] A. Blais, J. Gambetta, A. Wallraff, D. I. Schuster, S. M. Girvin, M. H. Devoret, and R. J. Schoelkopf, Quantum-information processing with circuit quantum electrodynamics, Phys. Rev. A **75**, 032329 (2007).
[46] S. Galliou, M. Goryachev, R. Bourquin, P. Abbé, J. P. Aubry, and M. E. Tobar, Extremely low loss phonon-trapping cryogenic acoustic cavities for future physical experiments, Sci. Rep. **3**, 2132 (2013).
[47] P. Kharel, Y. Chu, M. Power, W. H. Renninger, R. J. Schoelkopf, and P. T. Rakich, Ultra-high-Q phononic resonators on-chip at cryogenic temperatures, APL Photon. **3**, 066101 (2018).
[48] I. González Díaz-Palacio, M. Wenskat, G. K. Deyu, W. Hillert, R. H. Blick, and R. Zierold, Thermal annealing of superconducting niobium titanium nitride thin films deposited by plasma-enhanced atomic layer deposition, J. Appl. Phys. **134**, 035301 (2023).
[49] J. A. Valery, S. Chowdhury, G. Jones, and N. Didier, Dynamical sweet spot engineering via two-tone flux modulation of superconducting qubits, PRX Quantum **3**, 020337 (2022).
[50] C. K. Law and J. H. Eberly, Arbitrary control of a quantum electromagnetic field, Phys. Rev. Lett. **76**, 1055 (1996).
[51] S. Krämer, D. Plankensteiner, L. Ostermann, and H. Ritsch, QuantumOptics.jl: A Julia framework for simulating open quantum systems, Comput. Phys. Commun. **227**, 109 (2018).